



## **UWL REPOSITORY**

**repository.uwl.ac.uk**

Polarimetric alpha angle versus relative permittivity with dual-polarimetric GPR experiments

Zou, Lilong ORCID logoORCID: <https://orcid.org/0000-0002-5109-4866>, Tosti, Fabio ORCID logoORCID: <https://orcid.org/0000-0003-0291-9937>, Lantini, Livia ORCID logoORCID: <https://orcid.org/0000-0002-0416-1077> and Alani, Amir (2022) Polarimetric alpha angle versus relative permittivity with dual-polarimetric GPR experiments. In: 2021 11th International Workshop on Advanced Ground Penetrating Radar (IWAGPR), 01-04 Dec 2021, Valletta, Malta.

<http://dx.doi.org/10.1109/iwagpr50767.2021.9843156>

This is the Accepted Version of the final output.

UWL repository link: <https://repository.uwl.ac.uk/id/eprint/9383/>

**Alternative formats:** If you require this document in an alternative format, please contact: [open.research@uwl.ac.uk](mailto:open.research@uwl.ac.uk)

### **Copyright:**

Copyright and moral rights for the publications made accessible in the public portal are retained by the authors and/or other copyright owners and it is a condition of accessing publications that users recognise and abide by the legal requirements associated with these rights.

**Take down policy:** If you believe that this document breaches copyright, please contact us at [open.research@uwl.ac.uk](mailto:open.research@uwl.ac.uk) providing details, and we will remove access to the work immediately and investigate your claim.

# Polarimetric Alpha Angle versus Relative Permittivity with Dual-Polarimetric GPR Experiments

Lilong Zou  
School of Computing and Engineering  
University of West London  
London, U.K.  
lilong.zou@uwl.ac.uk

Livia Lantini  
School of Computing and Engineering  
University of West London  
London, U.K.  
livia.lantini@uwl.ac.uk

Fabio Tosti  
School of Computing and Engineering  
University of West London  
London, U.K.  
fabio.tosti@uwl.ac.uk

Amir M. Alani  
School of Computing and Engineering  
University of West London  
London, U.K.  
amir.alani@uwl.ac.uk

**Abstract**— Ground penetrating radar (GPR) is one of the most commonly used technologies for non-destructive testing (NDT). With the development of GPR signal processing methodologies, researchers are becoming more concerned not just with the detection of the target itself, but also with their physical properties and main features. In general, full waveform inversion algorithm is required to achieve this aim. But, full waveform inversion problem is a costive approach which need a huge computation. Thus, the ultimate goal of this study is to explore an effective strategy for estimating the relative permittivity of the target using polarimetric GPR data. We have investigated the relation between relative permittivity and polarimetric alpha angle based on the data collected by dual-polarization antennas GPR system. Laboratory experiments that measures different moisture sand targets (simulating for different relative permittivity target) in tree trunk holes have been carried out, taken as analog models for the physiological process representing decays in trees. After signal processing, the rough results that alpha angle versus with relative permittivity were obtained. The results show that for a dry sand the polarimetric alpha angle is small and the polarimetric alpha angle increases with increasing water content.

**Keywords**— *Polarimetric Alpha Angle, relative permittivity, tree trunk, dual-polarimetric, ground penetrating radar (GPR)*

## I. INTRODUCTION

As a recognised non-destructive testing (NDT) tool, Ground Penetrating Radar (GPR) is becoming increasingly common in the field of environmental engineering [1]–[6]. GPR is a real-time NDT technique that uses high-frequency radio waves to generate extremely high-resolution data in a limited time [7]. This technique uses electromagnetic (EM) waves which travel at a specific velocity determined by the permittivity of the material [8]. In a GPR measurement, a few wave characteristics, such as wavelength, frequency, amplitude, velocity and arrival time, are typically measured and used [7]. With the development of new GPR signal processing methodologies, finding information on the physical properties of hidden targets has become more important.

The main problem for the quantitative estimation of permittivity from GPR data lies in the inversion problems of the backscattered signal. Although a-priori object information and assumptions can be used to simplify the inversion problem, this is still a costly approach to implement. However, for many practical applications, approximate solutions have

proven to be sufficient. Empirical relations have been developed in the absence of any direct relationship between target parameters and backscattering signal models. Polarimetry plays here an important role as it allows either direct or parameterisation permittivity effects within the scattering problem in the remote sensing. The scattering problem of EM waves from surface targets has been an actual research topic over decades. Polarisation is also a property of EM waves that generally refers to the orientation of the electric field vector, which can be used to characterise target properties by polarimetric radar. Polarimetric decomposition is a type of polarimetric analysis methods, which can extract polarisation characteristics, that have been common in the terrain and land-use classification based on polarimetric synthetic aperture radar (SAR) data [9]–[11]. However, the technique has been less commonly used in the GPR community.

In this paper, we present an experiment to find whether the polarimetric information can be used to estimate the target permittivity. The aim is to evaluate backscattering amplitudes using dual-channel GPR data. This is based on the small perturbation scattering model (SPM) which described the scattering problem of EM waves from randomly rough surfaces. Some assumptions have been made in this paper to fit the Bragg-Model. First, the background medium is uniform, as a dry tree trunk specimen is used in this paper. Second, the target surface can be assumed as a rough surface in the measurement frequency range. In this regard, two holes with sand in the trunk are modelled. Last, the local incident angle of the EM wave to the target is close to 90 degrees. The reflection signals close to the hyperbolic curve peak were used for further processing. By measuring different moisture levels for sand materials filling holes in the trunk of known position and depth, a series GPR profiles were obtained. From the results, we could find that for a dry sand the alpha angle  $\alpha$  is small and increases with increasing sand moisture.

## II. METHODOLOGY

### A. Polarimetric Alpha Angle

In 1997, Cloude and Pottier proposed a method for the extraction of mean diffusion based on eigenvalues and eigenvectors decomposition of the coherence matrix. Based on this idea, they defined a set of parameters and called entropy and anisotropy parameters and alpha and beta angles.

The need for these parameters to identify objects in polarimetric radar images is used for the classification of fully polarimetric synthetic aperture radar (POLSAR) data [9].

For incoherent POLSAR data, Cloude-Pottier decomposition is developed based on the alpha-beta model. In the Cloude-Pottier decomposition, eigenvalue analysis is applied to the coherency matrix. Then, the coherency matrix is decomposed into three eigenvalues and corresponding eigenvectors. Each eigenvector is expressed in terms of the alpha-beta model.

Based on the polarimetric scattering model using the Bragg-Model,  $S_{VV}$  and  $S_{HH}$  are given by [10]-[11]:

$$S_{HH} = \frac{\cos \phi - \sqrt{\epsilon_r - \sin^2 \phi}}{\cos \phi + \sqrt{\epsilon_r - \sin^2 \phi}} \quad (1)$$

$$S_{VV} = \frac{(\epsilon_r - 1)(\sin^2 \phi - \epsilon_r(1 + \sin^2 \phi))}{(\epsilon_r \cos \phi + \sqrt{\epsilon_r - \sin^2 \phi})^2} \quad (2)$$

where  $\phi$  is the incident angle, and  $\epsilon_r$  indicated the relative permittivity. For Bragg Scattering, one may assume that there is only one dominant eigenvector and the eigenvector is given by:

$$k = \begin{bmatrix} S_{VV} + S_{HH} \\ S_{VV} - S_{HH} \\ 0 \end{bmatrix} \quad (3)$$

For a horizontal, slightly rough surface, the Cloude Pottier decomposition angle can be set to zero. With these constraints, we have:

$$\tan \alpha = \frac{|S_{VV} - S_{HH}|}{|S_{VV} + S_{HH}|} \quad (4)$$

where  $\alpha$  is the polarimetric alpha angle. In a real GPR survey, the local incident angle to a target can be assumed to be closed to 90 degree. In this case, the polarimetric alpha angle is a function of relative permittivity of the target.

### B. Radargram Pre-processing

The processing pipeline of this study consists of two sequential stages. A pre-processing algorithm is applied to increase the overall signal to clutter ratio. Subsequently, the alpha angle is estimated based on the formulation.

#### 1) Time-zero adjustment

Adjusting the initial position of surface reflection in GPR signals (the time when the radar pulse leaves the antenna and enters the ground is known as "zero time"). In order to adjust all traces to the zero-time position before any other processing methods are introduced, zero-time correction must be carried out.

#### 2) Background removal

Cross-coupling between the transmitter and the receiver as well as ringing noise and multiple reflections can mask the less dominant reflections from the target. In order to mitigate such clutter, the background removal (clutter rejection) method should be applied.

## III. LAB EXPERIMENT AND RESULTS

The lab experiment was carried out using the "Aladdin" dual polarised GPR system, manufactured by IDS Georadar (part of Hexagon). This GPR system is equipped with two 2GHz antennas polarised perpendicularly each to one another (HH and VV). The dual polarisation enables deeper surveying,

providing images of both shallow and deeper subsurface features. Standard antennas can detect shallow targets (e.g., rebars), but they cannot reveal features from deeper targets.

Figure 1 shows the dry tree trunk used in this experiment. For experimental purposes, two holes of around 15 cm depth and 1.5 cm radius were drilled into the trunk. Figure 1 (a) shows the empty holes, whereas Fig. 1 (b) shows the holes filled with sand. The radar system was then positioned on the side edge of the trunk, and circular measurements were collected by manoeuvring the GPR around it. The post-processing radargram is shown in Fig.2, where Fig. 2 (a) indicates the HH channel profile and Fig. 2 (b) indicates the VV channel profile. Two hyperbolic curves can be clearly seen from the profile. The color bar indicates the amplitude values of the signal in the radargram. It is observed that the reflection signal from the VV channel is weaker than the reflection signal from the HH channel.

The relative permittivity of the moisture sand was estimated based on the Topp equation [3][4].

$$\epsilon_r = 3.03 + 9.3\theta_w + 146\theta_w^2 - 76.7\theta_w^3 \quad (5)$$

where  $\theta_w$  is the moisture of sand and  $\epsilon_r$  indicates the relative permittivity.

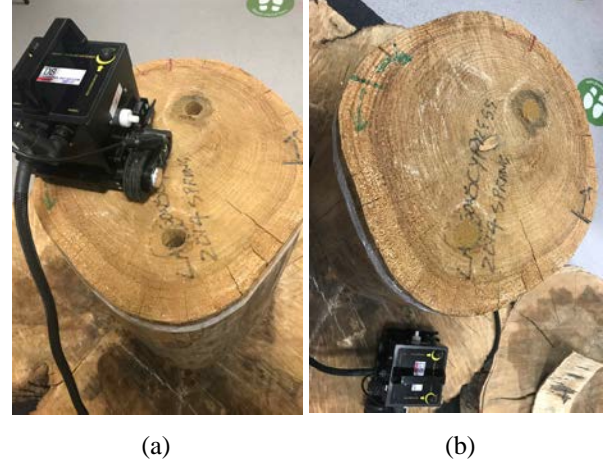


Fig. 1. Tree trunk with two holes; (a) empty holes; (b) holes filled with sand.

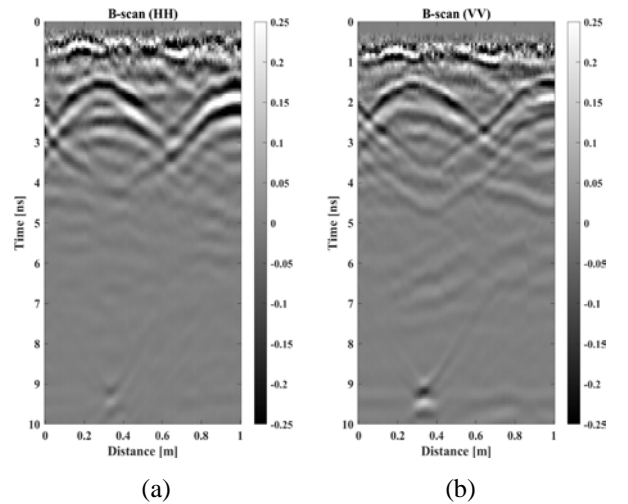


Fig. 2. Post-processed B-scan GPR profile of tree trunk; (a) HH channel B-scan; (b) VV channel B-scan.

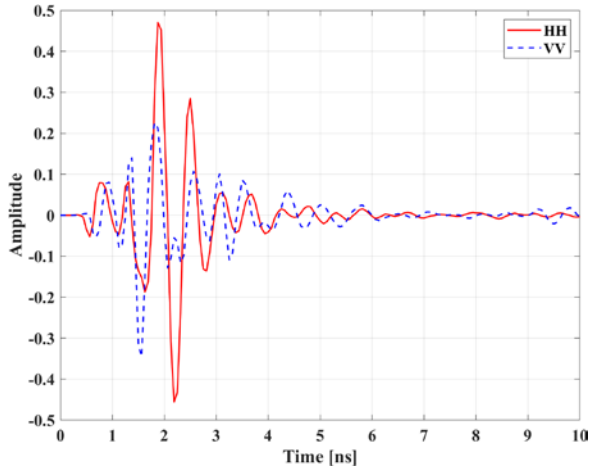


Fig. 3. A-scan of reflection signal obtained at the hyperbolic curve peak.

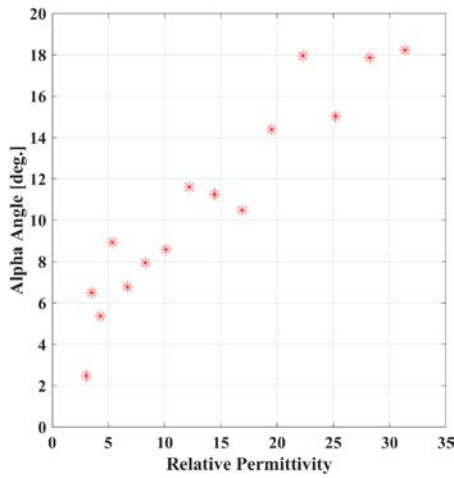


Fig. 4. Derivative of the Cloude-Pottier alpha angle with respect to the relative permittivity.

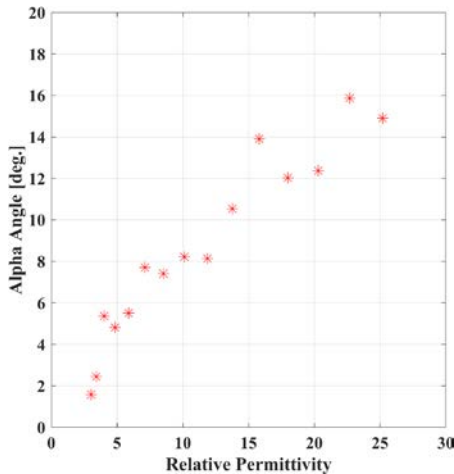


Fig. 5. Derivative of the Cloude-Pottier alpha angle with respect to the relative permittivity.

Regarding the control conditions of the moisture levels of the sand filling the two holes, dry sand was inserted in the beginning. The water content in sand was increased up to 45% in one hole, whereas it was brought up to 40% in the other hole. Totally, 15 GPR profiles were acquired in the

experiment. Fig. 3 shows the reflection signals obtained at the hyperbolic curve peak of each channel while the water content reached to 40%. The red line indicates the HH channel reflection, while the blue dash line indicates the VV channel reflection. The entire energy of the reflection will be calculated as  $S_{HH}$  and  $S_{VV}$  for further processing.

After calculation, the alpha angle versus the relative permittivity were plotted and shown in Fig.4 and Fig.5. The vertical axis indicates the alpha angle and the horizontal axis indicates the relative permittivity calculated by Equation 5.

From these two figures, we can conclude that for a dry sand the alpha angle  $\alpha$  is small and it increases with increasing water contents in the sand. In the lab experiment, it was not possible to provide an accurate relationship between the polarimetric alpha angle and the relative permittivity. However, for many practical applications, this approximate solution can be considered as a sufficient condition.

#### IV. CONCLUSIONS

In this paper the relation between the relative permittivity and the Cloude-Pottier alpha angle based on dual-polarimetric GPR data is investigated. The derivations and experimental results show that the relative permittivity is strictly related to the Cloude-Pottier alpha angle. Outcomes also show that for a low relative permittivity, the alpha angle  $\alpha$  is small, and that the angle increases with increasing relative permittivity.

#### REFERENCES

- [1] L. Zou, L. Yi and M. Sato, "On the Use of Lateral Wave for the Interlayer Debonding Detecting in an Asphalt Airport Pavement Using a Multistatic GPR System," *IEEE Trans. Geo. Remote Sens.*, vol. 58, no. 6, pp. 4215-4224, June 2020.
- [2] L. Zou, K. Kikuta, A. M. Alani and M. Sato, "Study on Wavelet Entropy for Airport Pavement Debonded Layer Inspection by using a Multi-Static GPR System," *Geophys.*, vol. 86, no. 3, pp. WB69-WB78, May/June 2021.
- [3] L. Zou, Y. Wang, I. Giannakis, F. Tosti, A. M. Alani and M. Sato, "Mapping and Assessment of Tree Roots using Ground Penetrating Radar with Low-Cost GPS," *Remote Sens.*, vol. 12, no. 8, pp. 1300, April 2020.
- [4] A. Benedetto, F. Tosti, B. Ortuani, M. Giudici and M. Mele, "Soil moisture mapping using GPR for pavement applications," *7th International Workshop on Advanced Ground Penetrating Radar*, 2013, pp. 1-5.
- [5] A. M. Alani, I. Giannakis, L. Zou, L. Lantini and F. Tosti, "Reverse-Time Migration for Evaluating the Internal Structure of Tree-Trunks Using Ground-Penetrating Radar," *NDT&E Int.*, vol. 115, pp. 102294, October 2020.
- [6] A. M. Alani, F. Soldovieri, I. Catapano, I. Giannakis, G. Gennarelli, L. Lantini, G. Ludeno and F. Tosti, "The Use of Ground Penetrating Radar and Microwave Tomography for the Detection of Decay and Cavities in Tree Trunks," *Remote Sens.*, vol. 11, no. 18, pp. 2073, September 2019.
- [7] D. J. Daniels, *Ground Penetrating Radar*, 2nd ed. London, U.K.: IEE Press, 2004.
- [8] H. M. Jol, *Ground Penetrating Radar: Theory and Applications*, The Netherlands, Amsterdam: Elsevier, 2009.
- [9] S. R. Cloude and E. Pottier, "A review of target decomposition theorems in radar polarimetry," *IEEE Trans. Geosci. Remote Sens.*, vol. 34, no. 2, pp. 498-518, Mar. 1996.
- [10] J. Lee and E. Pottier, *Polarimetric Imaging: From Basics to Applications*, FL, Boca Raton: CRC Press, 2009.
- [11] J. van Zyl and Y. Kim, *Synthetic Aperture Radar Polarimetric*, NJ, Hoboken: Wiley, 2011.